DEVELOPING A NOVEL FIELD-BASED COMPACTIVE VISCOMETER

INTERNATIONAL SNOW SCIENCE WORKSHOP 2026, WHISTLER CANADA

Benjamin H. Silberman[1]*, Eric R. Pardyjak[1], Ashley Spear[1], Dhiraj K. Singh[1]

1 University of Utah, Salt Lake City, UT, USA
** Indicates the presenting author*

ABSTRACT: Accurate prediction of storm-snow instability requires understanding how snow density (ρ_s) evolves during active snowfall, yet key mechanical properties such as compactive viscosity (η_s) remain understudied due to limited in situ observations. Compactive viscosity governs the rate of densification and directly influences snow stability and avalanche propagation, but existing parameterizations rely primarily on laboratory data or post-storm measurements that do not capture natural storm conditions. A framework is proposed to evaluate η_s using a Differential Emissivity Imaging Disdrometer (DEID), which measures snow density and microstructural properties on a snowflake-by-snowflake basis, enabling a physics-based parameterization of densification in real time. To accomplish this, we present a novel field-based viscometer designed to measure η_s of freshly fallen snow during and immediately after storms. Due to anomalous weather conditions during the 2025–2026 winter season, the dataset of in situ viscosity measurements is currently limited. Preliminary results therefore focus on instrument development, calibration, and the theoretical framework linking strain rate, applied stress, and densification. These results will demonstrate the feasibility of capturing real-time rheological behavior in low-density storm-snow and establish the methodology for future data collection. Ongoing and future work will expand the dataset during the 2026–2027 winter season and integrate viscosity parameterizations into a broader avalanche forecasting framework. Specifically, η_s-derived densification models will be incorporated into a coupled shear and anticrack stability system, enabling improved prediction of storm-snow instability using both real-time observations and numerical weather prediction. This research addresses a critical gap in avalanche science by using a novel field measurement technique for storm-snow densification and providing a pathway toward remotely operated physics-based forecasting tools.

KEYWORDS: compactive viscosity, storm snow, densification, DEID, snow mechanics

1. INTRODUCTION

Forecasting avalanches that release within storm-snow requires knowing how the density (ρ_s) of freshly fallen snow evolves as the storm progresses. Models that quantify snowpack instability rely on the shear strength (Σ_s), or the critical fracture energy of storm-snow (G_{I_c}), both which are driven by ρ_s. This suggests that the timing of instability depends on the rate at which storm-snow densifies.

Operational models describe the densification rate with a linear viscous law proposed by Kojima (1967), in which strain rate ($\dot{\epsilon}$) is proportional to the overburden stress (σ), with compactive viscosity (η_s) acting as the constant of proportionality. This linear model is well supported for the snow it was calibrated on – buried layers whose ρ_s is between 100-500 kg m^{-3} – and reproduces seasonal settlement well.

* Corresponding author address:
Benjamin H. Silberman, University of Utah,
Salt Lake City, UT 84116;
tel: +1 781-234-4125
email: b.silberman@utah.edu

Unfortunately, η_s is difficult to determine. Parameterizations of η_s are typically written as a function of density and temperature multiplied by an empirical coefficient, C_0, that coefficient is known to vary substantially between snowfalls without a solid explanation. Endo et al. (1990) reported a fourfold spread in their coefficient and attributed it to snow temperature and crystal type at deposition but could not separate the two. The influence of snow microstructure on densification in typical models is captured by this empirical coefficient C_0.

Two approaches to measuring snow densification have been established, and neither account for storm-snow microstructure. Field studies that use an undisturbed snowpack and take σ as whatever the snowstorm deposits were unable to quantify snowpack qualities outside of ρ_s (Endo et al., 1990; Kajikawa and Ono, 1990). Laboratory studies control σ, but disturb samples from the natural environment. Schleef et al. (2014) sieved their samples, while Chernov (2024) repacked theirs. In each of these cases, the snow's bond networks are disrupted, which are understood to govern mechanics (Bernard et al., 2022).

https://doi.org/10.15788/1790098953

This paper describes an instrument designed to merge these two approaches: applying a controlled and variable load to an undisturbed column of snow during active storm events. For the upcoming 2026-2027 winter season, this instrument will be used alongside a Differential Emissivity Imaging Disdrometer (DEID), measuring the microstructure of the snow as it falls (Singh et al. 2021). Here we do not present field measurements, as anomalous conditions during the 2025–2026 season limited in-situ data collection. Instead, we describe the instrument design, the measurement methodology, and a demonstration on a compliant proxy medium of the initial-compression measurement.

2. BACKGROUND

2.1 *Constitutive framework*

Following the work of Kojima (1954; 1967), the compactive strain rate $\dot{\epsilon}$ of a layer of snow of thickness h, at time t, and density ρ_s is given by

$$\dot{\epsilon} = -\frac{1}{h}\frac{dh}{dt} = \frac{1}{\rho_s}\frac{d\rho_s}{dt}. \tag{1}$$

The question becomes how $\dot{\epsilon}$ relates to the load σ exerted by additional snow. Kojima (1954) sought this answer by compressing snow in the laboratory under constant uniaxial stress and found $\dot{\epsilon}$ is proportional to σ for loads below 30 g cm^{-2} (2942 Pa). Writing the constant of proportionality as the compactive viscosity η_s, we get

$$\dot{\epsilon} = \frac{\sigma}{\eta_s}, \qquad \eta_s = \frac{\sigma}{\dot{\epsilon}}. \tag{2}$$

Equation 2 defines the measurement principle of the proposed instrument: a known applied stress and a resolved rate of height change give η_s directly. It also assumes a linear relationship between $\dot{\epsilon}$ and σ, in which η_s is fixed by the state of the snow and independent of the load applied. Recent work that has investigated the behavior of storm-snow consistently found this response to be non-linear, taking a power-law form proposed by Glen (1955);

$$\dot{\epsilon} = \dot{\epsilon_0}\left(\frac{\sigma}{\sigma_0}\right)^m, \tag{3}$$

with a reported stress exponent range of $m = 1.8$ to 4 (Védrine and Hagenmuller, 2026). In Eq. 3, $\dot{\epsilon_0}$ = 1 s^{-1}, and σ_0 is a reference stress. When this relation is not linear, η_s depends in part on the load at which it was measured.

Applying the linear relation in the field, Kojima (1967) found viscosity to rise exponentially with density,

$$\eta_s = Ce^{k\rho_s}, \tag{4}$$

with $k \approx 21$ cm³ g^{-1}, over a density range of 100–500 kg m^{-3}. Conway and Wilbour (1999) use the same exponential with the density normalized by that of ice, B_2 = 19.3, which recovers Kojima's coefficient exactly. Endo et al. (1990) found that Eq. 4 breaks down below ~110 kg m^{-3}, and that snow with relatively low ρ_s is better described by a power law,

$$\eta_s = C\rho_s^4, \tag{5}$$

which applies with one set of coefficients from 50 kg m^{-3} up to approximately 300 kg m^{-3}. Abe (2001) added a temperature dependence to the coefficient, $C = 0.21e^{-0.166T_s}$, where T_s is snow temperature in °C. Because snow deforms by thermally activated processes at the grain bonds, this dependence is more commonly expressed in Arrhenius form (Hayes et al., 2004),

$$\eta_s = C_0\rho_s^4 e^{\frac{E}{RT_k}}, \tag{6}$$

where E is the activation energy, R the gas constant, and T_k the absolute temperature of snow in °K. The leading coefficient C_0 carries whatever influences η_s beyond ρ_s and T_k.

Combining this viscous densification law with a metamorphic contribution σ_m added to the overburden σ_s, the SNOw Slope Stability model (SNOSS) (Hayes et al., 2004; Conway and Wilbour, 1999) expresses the evolution of density as

$$\frac{1}{\rho_s}\frac{d\rho_s}{dt} = \frac{\sigma_m + \sigma_s}{\eta_s}. \tag{7}$$

Equations 1-7 form the framework used in this study.

2.2 *Uncharacterized microphysics in C_0*

Within this framework, the density exponent and the activation energy in Eq. 6 are understood to reflect the bulk deformation physics of ice and are commonly treated as material constants; n = 4 (Endo et al., 1990) and E = 67.3 kJ mol^{-1} (Conway and Wilbour, 1999). What remains uncertain is C_0.

Table 1: Loading and sample handling across published methods.

Study	*Load applied by*	*Snow condition*
Kojima (1967), Endo et al. (1990), Kajikawa and Ono (1990)	Natural accumulation	Undisturbed, in place
Kojima (1967)	Snow blocks added and removed by hand	Undisturbed, in place
Casson et al. (2008), Schleef et al. (2014), Chernov (2024)	Calibrated weights	Field-collected, transferred to container
Abe (2001)	Calibrated weights	Laboratory-grown
This study	**Calibrated weights**	**Undisturbed, unconfined, in-place**

Endo et al. (1990) reported values of their coefficient C (Eq. 5) spanning 0.193 to 0.794 N s m^{-2} (m^3 kg^{-1})^4, a factor of four, and attributed the spread to snow temperature and to the crystal form present at deposition. Kajikawa and Ono (1990) subsequently isolated the crystal-form effect directly, measuring new snow layers every six hours and finding that spatial dendrites are approximately five times more viscous than stellar crystals *at the same density*, with plates and rimed forms falling between. It is therefore well understood that ρ_s alone does not determine η_s.

Rearranging Eq. 6, we can solve for C_0, where these microstructures reside;

$$C_0 = \frac{\eta_s}{\rho_s^4\, e^{\frac{E}{RT_k}}}, \tag{8}$$

so that a measured η_s, ρ_s and T_k, yields C_0 for each observation. Kojima (1967) reached the same conclusion from his own data, noting a scatter of η_s at a given ρ_s, which could be explained by grain size. In more modern parameterization, Kojima's noted dependency is absorbed into C_0. Until recently, this physical parameterization could not be observed directly during a storm. Because of the DEID, this work will not only measure the needed parameters to solve Eq. 8 but investigate whether this relationship still holds for storm-snow.

2.3 Characterizing C_0 with the DEID

The Differential Emissivity Imaging Disdrometer (DEID) measures the mass, size, shape and ρ_s of individual hydrometeors as they fall, using a temperature-controlled hotplate of low emissivity observed by an infrared camera (Singh et al., 2021; Singh et al. 2024). From the thermal image sequence, the contact area A_s and melting behavior of each particle give its mass and ρ_s on a snowflake-by-snowflake basis.

Two dimensionless descriptors of particle geometry follow from these DEID measurements (Morrison et al., 2023, Silberman et al. 2026). Shape density index (SDI) is a metric that compares a snowflake's projected cross-sectional area to the area an equivalent melted water droplet would occupy, quantifying departure from compact geometry at constant mass. Complexity (Cx) is a metric that compares the area of the circumscribing rectangle to the snowflake's own area, capturing angularity and the potential for interparticle interlocking. Both SDI and Cx quantify aspects of snowflake microphysics (Donovan et al., 2025).

The proposed method in this paper therefore has two distinct components. The viscometer measures η_s for an undisturbed column of storm-snow under a known load, while the DEID, operating on the same falling snow, quantifies density as well as the microstructural descriptors SDI and Cx. C_0 is determined from field-measurements of η_s and Eq. 8 and is regressed against DEID-measured parameters to determine a functional relationship $C_0 = f(\phi_{DEID})$, where ϕ is a vector of dimensionless physical properties. If such a relationship can be established, η_s becomes predictable in real time from remotely sensed quantities, with the exponent and activation energy held as material constants.

2.4 Summary of current literature

Védrine and Hagenmuller (2026) directly state in their findings: "repeated experiments under perfectly controlled conditions (e.g. changing the applied stress without altering any parameter that affects the reference stress σ_0) are seldom conducted and are challenging on snow". Measuring η_s in a way that supports Eq. 7 requires varying σ while holding ρ_s, T_k and microstructure at their natural condition, and being able to measure that microstructure independently. Existing methods do one or the other and are summarized in Table 1.

In field studies, σ is determined by the water equivalent of the accumulating snowpack. Kojima's (1967) trenching remains the closest approach to a controlled-load test on undisturbed snow, though the increments were coarse and manual, with layer thicknesses compared days apart. Laboratory studies control the applied σ but require the snow to be moved into a sample holder, transferred (Casson et al., 2008), sieved (Schleef et al., 2014), or repacked (Chernov, 2024), which disrupts the bond network through which load-driven creep acts (Bernard et al., 2022). Neither approach quantifies snowflake microstructure. Obtaining C_0 for freshly fallen storm-snow therefore requires controlled, variable loading applied to an unconfined column of undisturbed snow, observed alongside an instrument capable of resolving the microstructure of the snow forming that column.

3. COMPACTIVE VISCOSITY INSTRUMENT DESIGN

Here we present a viscometer, pictured in Fig. 1, designed to measure η_s in the field.

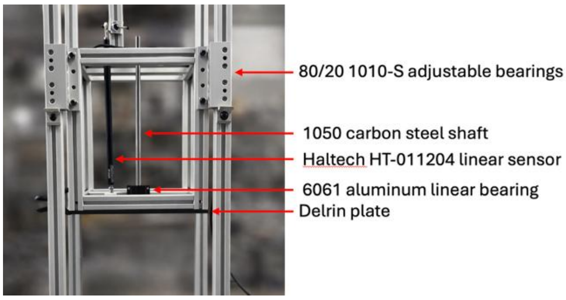

Figure 1: Photograph of the University of Utah field viscometer in a laboratory setting.

The horizontal load plate is a 24 × 24 cm plate of 0.68 cm Delrin, giving a bearing area of 576 cm²; Delrin was selected for stiffness, dimensional stability and low moisture absorption. It is carried on a 1050 carbon steel shaft, 31.75 cm long and 0.9525 cm in diameter, running through a 6061-aluminum linear bearing that constrains the plate to vertical translation while contributing negligible friction. The viscometer is mounted in a 27 × 24 × 24 cm frame of 80/20 1010-S extrusion, carried on 150 cm uprights via single-flange bearing brake kits so the assembly can be set to the snow surface.

The plate itself imposes a 118.8 Pa axial load while calibrated weights placed on the plate increase σ in a controlled fashion. This fits within the range used in published snow work. For example, Kajikawa and Ono (1990) used a range of 5.9 to 157 Pa, Schleef et al. (2014) 0 to 318 Pa, Chernov (2024) 0.1 to 3.8 kPa. Our field-based anticipated loads are all below Kojima's (1954) linearity limit of 2942 Pa.

The snowpack column height is recorded at ~40 Hz, by a Haltech HT-011204 linear position sensor coupled to the plate shaft and read through a LabJack T7-Pro data acquisition device. The Haltech linear position sensor was calibrated against manual measurements by piecewise interpolation over 21 points spanning 0-200 mm at 10 mm intervals, with readings outside that span flagged at acquisition. Snowpack displacement is measured directly from a known initial height of h_0 and plate displacement:

$$h(t) = h_0 + [x(t_0) - x(t)]. \tag{9}$$

From Eq. 9, the time resolved snowpack displacement gives $\dot{\epsilon}$ from Eq. 1. Thus, by knowing the load applied σ, η_s is readily solved for using Eq. 2.

4. METHODS

4.1 *Laboratory testing with a proxy*

To simulate the compression of storm-snow in the lab, lightweight decorative gift paper was lightly crumpled and placed inside a column (Fig. 2). These 'snow columns' were built to heights of 114-265 mm on top of a flat surface.

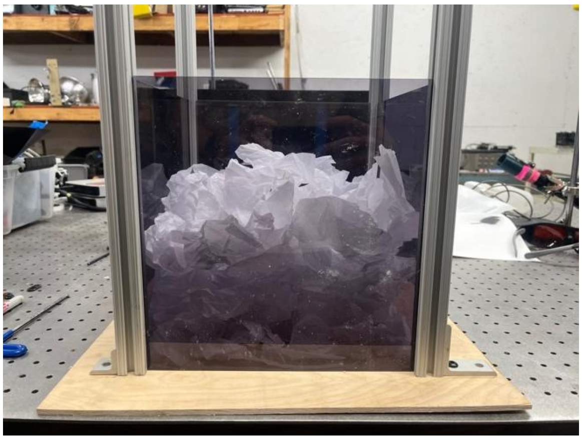

Figure 2: A column of loosely-packed decorative gift paper, simulating a freshly deposited snowpack.

This proxy is not a mechanical analogue for storm snow and is not treated as one. Its purpose instead is to exercise the complete measurement chain; sensing, acquisition, timing and data reduction. The lightweight decorative gift paper density was 4.3–6.5 kg m⁻³, which is more than an order of magnitude less than new snow. As a result, the plate collapses the column more rapidly than it would real snow. Published loading of new snow at comparable stresses does not produce this behavior — Schleef et al. (2014) loaded up to 318 Pa, Abe (2001) at 22–279 Pa and Kajikawa and Ono (1990) at 5.9–157 Pa. Each of these report continuous creep at 10^{-6} to 10^{-5} s⁻¹. Thus, we do not anticipate this to be the case in the field, where the plate would expect to initiate a creep load.

4.2 Loading protocol and data reduction

The testing is initialized by lowering the plate to the undisturbed surface and released. The position is then logged continuously from immediately before release until the column comes to rest. The interval of interest is the initial compression the column undergoes; this is the first response of material that contains its naturally deposited ρ_s and microstructure. After this initial compression, the material becomes compressed and can no longer be considered 'fresh'.

A subsample of the time series of data was used to compute compactive viscosity. A compression window is defined for every test run as follows: it starts immediately before the start of the plate's descent and ends at the height where the plate stops. A least-squares line is fit to *h(t)* over that window, giving

$$\dot{\epsilon} = -\frac{1}{\bar{h}}\frac{dh}{dt}, \qquad (10)$$

where the overbar denotes the mean over the window. All computations use g = 9.8 m s⁻².

5. RESULTS

5.1 Initial compression of the proxy

Three tests were performed, releasing the plate onto a freshly-built proxy column of 170.0 mm (Test 1) or 265.0 mm (Tests 2 and 3), at densities of 6.0, 6.5 and 4.30 kg m⁻³. The applied σ was 118.8 Pa (the weight of just the plate) in each of the three tests and was held constant throughout each trial.

Figure 3 shows Test 3 with the data processed as described in Section 4.2. In the upper panel the "fitting window" is shown within the full-time series. The lower panel shows the isolated window with its best fit line. Figure 4 shows all three trials with their fits. The columns were built by hand and are not replicates; Tests 1 and 2 compress by 49.9% and 39.0% in a single event, while Test 3 compresses in a sequence of smaller steps of which the fitted window is one, spanning 11.5%.

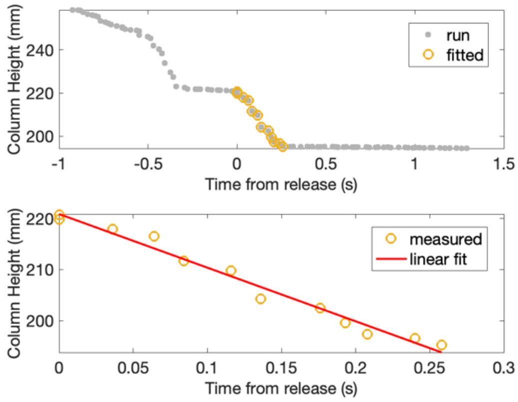

Figure 3: Upper: Complete time series with the "fitting window" shown as orange-colored circles. Lower: "fitting window" alone with least-squares line.

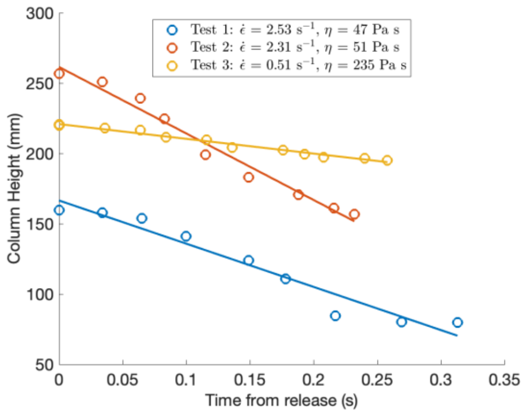

Figure 4: Initial compression of all three proxy columns under the plate, with the fit of Eq. 10 overlaid on each.

5.2 Interpretation of proxy results

The three trials demonstrate the measurement methodology end to end: a known stress applied to an confined column, a continuously recorded compression from release to arrest, and η_s recovered from Eq 2. These results establish nothing about the deformation of snow, simply the performance of the device. At $\dot{\epsilon}$ of 0.5–2.5 s⁻¹ the proxy is five orders of magnitude faster than any published snow measurement and far above the 4×10⁻⁴ s⁻¹ threshold below which Védrine and Hagenmuller (2026) admit tests as viscoplastic.

From an instrument characterization perspective, the three trials indicate that sensing, acquisition, timing and reduction should all work work for real snow. When run alongside the DEID, the resulting η_s values will be fed into Eq. 8, to regress C_0 against DEID-measured parameters. This will allow our viscometer to not only measure η_s directly, but to also model its behavior in relation to storm-snow microstructure.

6. SUMMARY AND FUTURE WORK

We have described and lab-tested a field-based compactive viscometer intended to measure η_s for undisturbed storm-snow. Lab tests were conducted to simulate the use of the viscometer and characterize its response on lightweight decorative gift paper in a laboratory setting. Three initial-compression tests recovered out-of-expected-range strain rates due to the proxy's low density (ρ_s = ~4.3-6.5 kg m^{-3}) yet demonstrated the viscometer's potential for field measurements. Furthermore, we showed that, when applying the proposed methodology (controlling σ, leaving the material in its undisturbed state) to literature-based storm-snow, we expect η_s values of 10^7–10^8 Pa s at densities of 70–120 kg m^{-3}.

Determining C_0 requires the field-measured η_s, which was the limit of our proxy testing. Starting with the upcoming 2026-2027 season at the Atwater Snow-Study Plot, we will follow the methodology presented herein; releasing the plate onto undisturbed columns of storm-snow at a fixed applied stress, with a co-located DEID recording SDI, and Cx of the ongoing storm event. Each pairing yields η_s from Eq. 2 and C_0 from Eq. 8. The resulting C_0 values will be regressed against the DEID descriptors to seek a functional form $\mathrm{C}_0 = f(\phi_{\mathrm{DEID}})$.

Endo et al. (1990) reported a fourfold spread in this coefficient and attributed it to temperature and crystal form without being able to separate them; Kajikawa and Ono (1990) isolated the crystal-form effect but could not observe it during active storms. The DEID can measure these physical properties during active deposition. Establishing the relationship would make η_s predictable in real time from remotely sensed quantities in near-real-time, supplying the densification term to aid in forecasting for storm-snow instabilities.

Beyond C_0, this instrument has the potential to settle the uncharacterized relationship between $\dot{\epsilon}$ and σ, believed to behave differently in storm-snow. Because the plate and its weights apply a known and adjustable σ, a column measured at one load can be measured again at a second. The two resulting $\dot{\epsilon}$ give the stress exponent present in Eq. 3 directly for an observed layer of storm-snow. This is the controlled-loading test Védrine and Hagenmuller (2026) identify as absent from the literature – "repeated experiments under perfectly controlled conditions ... are seldom conducted and are challenging on snow" – and it would establish whether the proportionality assumed in Eq. 2 holds for storm-snow.

COMPETEING INTERESTS

The DEID® and Particle Flux Analytics® are registered trademarks. The authors declare the following financial interests and/or personal relationships, which may be considered potential competing interests:

TJG is a scientific advisor for Particle Flux Analytics and holds an equity interest. TJG, DKS, and ERP are named patent holders for the DEID® (No. 11,674,878), which is licensed to Particle Flux Analytics®. ERP and DKS have royalty interest in DEID® sales.

ACKNOWLEDGEMENTS

We thank Steven Clark of the Utah Department of Transportation (UDOT) for his continued support and direction throughout each winter season. We thank Allan Reaburn and his colleagues at Particle Flux Analytics, Inc. for their contributions to the development and advancement of the DEID. This material is based upon work primarily supported by the American Avalanche Association (AAA) research grant.

REFERENCES

Abe, O., 2001. Creep experiments and numerical simulations of very light artificial snowpacks, Ann. Glaciol., 32, 39–43.

Bernard, A., Hagenmuller, P., Montagnat, M., and Chambon, G., 2022. Disentangling creep and isothermal metamorphism during snow settlement with X-ray tomography, J. Glaciol.,68(276),899–910, https://doi.org/10.1017/jog.2022.109.

Casson, J., Stoelinga, M., and Locatelli, J., 2008. Evaluating the importance of crystal-type on new snow instability: a strength vs. stress approach using the SNOSS model, in: Proceedings of the International Snow Science Workshop, Whistler, BC, 21–27 September 2008, 612–618.

Chernov, R. A., 2024. Experimental determination of the coefficient of viscosity of the dry snow, Led i Sneg (Ice and Snow),64(2),273–280,https://doi.org/10.31857/S2076-673424020106.

Conway, H. and Wilbour, C., 1999. Evolution of snow slope stability during storms, Cold Reg. Sci. Technol., 30, 67–77.

Donovan, S., D.K. Singh, T. Garrett, and E.R. Pardyjak, 2025. Quantification and parameterization of snowflake fall speeds in the atmospheric surface-layer, Atmos. Chem. Phys., 25, 16729–16746, https://doi.org/10.5194/acp-25-16729-2025.

Endo, Y., Ohzeki, Y., and Niwano, S., 1990. Relation between compressive viscosity and density of low-density snow, Seppyo, J. Jpn. Soc. Snow Ice, 52(4), 267–274 (in Japanese with English summary).

Glen, J. W.: The Creep of Polycrystalline Ice, Proceedings of the Royal Society of London Series A, 228, 519–538, https://doi.org/10.1098/rspa.1955.0066, 1955.

Hayes, P., Wilbour, C., Gibson, R., Marshall, H. P., and Conway, H., 2004. A simple model of snow slope stability during storms, in: Proceedings of the International Snow Science Workshop, Jackson Hole, WY, 165–171.

Kajikawa, M. and Ono, N., 1990. Relationship between compactive viscosity of new snow and the crystal shape of snowfall, Seppyo, J. Jpn. Soc. Snow Ice, 52(4), 283–287 (in Japanese with English summary).

Kojima, K., 1954. Visco-elastic properties of snow, Low Temp. Sci., A12, 1–13 (in Japanese with English summary).

Kojima, K., 1967. Densification of seasonal snow cover, in: Physics of Snow and Ice, edited by: Ōura, H., Institute of Low Temperature Science, Hokkaido University, Sapporo, 1(2), 929–952.

Morrison, T. J., Meisenheimer, T., Garrett, T., Singh, D., Donovan, S., and Pardyjak, E., 2023. Relating storm-snow avalanche instabilities to data collected from the Differential Emissivity Imaging Disdrometer (DEID), Cold Reg. Sci.Technol.,210,103839, https://doi.org/10.1016/j.coldregions.2023.103839.

Schleef, S., Löwe, H., and Schneebeli, M., 2014. Influence of stress, temperature and crystal morphology on isothermal densification and specific surface area decrease of new snow,TheCryosphere,8,1825–1838, https://doi.org/10.5194/tc-8-1825-2014.

Silberman, B. H., Morrison, T. J., Singh, D. K., Garrett, T. J., and Pardyjak, E. R., 2026. Optimizing the Gibson-Ashby model to predict the shear strength of storm-snow, unpublished manuscript.

Singh, D. K., Donovan, S., Pardyjak, E. R., and Garrett, T. J., 2021. A differential emissivity imaging technique for measuring hydrometeor mass and type, Atmos. Meas. Tech., 14, 6973–6990, https://doi.org/10.5194/amt-14-6973-2021.

Singh, D. K., Pardyjak, E. R., and Garrett, T. J., 2024. Time-resolved measurements of the densities of individual frozen hydrometeors and fresh snowfall, Atmos. Meas. Tech., 17, 4581–4598, https://doi.org/10.5194/amt-17-4581-2024.

Védrine, L. and Hagenmuller, P., 2026. Revisiting snow settlement with microstructural knowledge, The Cryosphere, 20, 1257–1277, https://doi.org/10.5194/tc-20-1257-2026.